Iranian Journal of Mathematical Chemistry

IJMC

DOI: 10.22052/IJMC.2023.247422.1653
Vol. 14, No. 1, 2023, pp. 55-64
Research Paper

Finding the $V_2(555-777)$ Double Vacancy Defect in Graphene Using Rotational Symmetry

Margaret Lyn Archibald[1*], Sonja Currie[1] and Marlena Nowaczyk[2,3]

[1]The John Knopfmacher Centre for Applicable Analysis and Number Theory, School of Mathematics, University of the Witwatersrand, Private Bag 3, P O WITS 2050, South Africa

[2]AGH University of Science and Technology, Faculty of Applied Mathematics, al. A. Mickiewicza 30, 30-059 Krakow, Poland

[3]Halmstad University, School of Information Technology, Box 823, 301 18 Halmstad, Sweden

Keywords:

Periodic orbit,
Double vacancy defect,
Rotational symmetry,
Graphene,
Inverse problem

AMS Subject Classification (2020):

92E10; 81Q10; 47N60

Article History:

Received: 25 August 2022

Accepted: 5 May 2023

Abstract

We use the underlying hexagonal structure of graphene to identify uniquely the position pertaining to a divacancy defect of type $V_2(555-777)$. This is achieved by considering at most three closed path readings and the symmetry of the defective structure. We work in the corresponding rectangular model but still rely on the rotational symmetry of the original hexagonal grid. Our approach is purely mathematical and therefore there is no need for imaging technologies.

1 Introduction

The two-dimensional honeycomb structure of pristine (defect-free) graphene is a one-atom-thick layer of covalently-bonded carbon atoms. Graphene exhibits important mechanical, electrical, thermal and optical properties which lead to applications in various fields such as electronics (batteries, transistors and sensors) and even in the process of gas purification.

When a graphene nano-ribbon contains defects, it affects the properties of the material which can influence its performance, for example in graphene-based nanodevices. There are several existing methods to detect defects in graphene but many are expensive or complicated to implement. Our approach uses inverse spectral theory with the advantage that it avoids imaging technologies such as reflectance mapping, Raman imaging, transmission electron microscopy (TEM) or scanning tunneling microscopy (STM). The authors of [1] give an alternative approach by observing the thermal vibration properties of a graphene sheet and then detecting the break using machine learning.

*Corresponding author
E-mail addresses: margaret.archibald@wits.ac.za (M. Archibald), sonja.currie@wits.ac.za (S. Currie), marlena17nowaczyk@gmail.com (M. Nowaczyk)
Academic Editor: G. H. Fath-Tabar

In [2], the authors evaluate the effects of structural defects on the Young's modulus of graphene. This is done by using molecular dynamics (a computer simulation method for analyzing the physical movements of atoms and molecules) to obtain information about the underlying structures.

A review of defects in graphene together with atomic images can be found in [3] or [4]. In [5] we identified the position of a single vacancy (SV) defect and then extended the analysis to the Stone-Wales SW(55-77) and the double vacancy $V_2(5-8-5)$ defects in [6].

The particular defect that we consider in this paper occurs when a piece of graphene has two adjacent nodes missing in such a way that three pentagons and three heptagons are formed and alternated in a clockwise circle. This divacancy defect is called $V_2(555-777)$ and its graphical depiction is given in Figure 1.

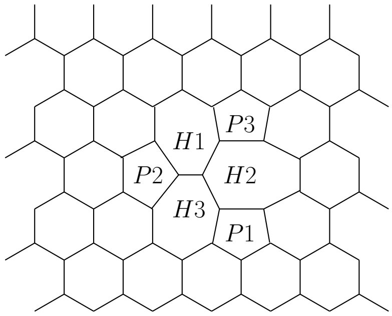

Figure 1: Hexagonal grid with a $V_2(555-777)$ defect

A mathematical representation of graphene is given by a quantum graph as follows. The carbon atoms are denoted by the nodes and the bonds by edges, each of length one, creating a metric graph. The movement of low energy free electrons in the structure can be modelled by the Laplace equation together with Kirchhoff boundary conditions at the nodes. The lengths of the closed paths in the graph and the eigenvalues (spectrum) of the Laplace operator are related to each other by the trace formula see [7, 8]. Thus, by reading the spectrum from a detector we can determine almost all the lengths of closed paths in the graph model. Note that defects in the grid cause changes in the spectra.

We show that the position of this defect can be uniquely identified using at most three readings using a detector to measure the lengths of closed paths from each point. The fact that the new polygons have an odd number of sides is crucial, as this leads to closed paths of odd length starting at the point where the detector is placed, travelling around a pentagon/heptagon, and then ending back at the detector. Note that the absence of closed paths of odd length does not necessarily indicate that the graphene has no defects since some defects do not result in polygons with an odd number of sides.

The structure of the paper is as follows. In Section 2 we depict the $V_2(555-777)$ defect in the rectangular grid. Depending on the length (modulo 4) of the shortest closed path of odd length from the detector, round part of the defect and back again, we partition the rectangular grid into 12 distinct regions. Moreover, we identify the region in which the detector was originally placed. In Section 3 we discuss the symmetry of the defect within the hexagonal structure and consequently how this translates to the rectangular grid. We divide the regions into three (equivalent) groups in order to take advantage of this symmetry in our analysis. We introduce an algorithm for locating the coordinates of the center node of the defect relative to the first reference point (first position of the detector) for nodes in the base group in Section 4. Due to the symmetry explained in the previous section, this is sufficient for finding the defect from any given reference point in the grid. The algorithm is illustrated in Section 5 by an example.

2 The $V_2(555-777)$ defect

The hexagonal grid is transformed to a rectangular grid resembling a brick wall on an (x, y) coordinate system. As noted in [5] this distortion is a compression in the vertical direction causing the non-vertical lines to become horizontal. Therefore, we can use the (x, y) coordinate system to reference the nodes on the grid more easily.

The $V_2(555-777)$ break is modelled by three pentagons and three heptagons as shown by the shaded region in Figure 2. On the rectangular grid, this is obtained by one brick disappearing and being replaced by a single vertex (where $H1$, $H2$, $H3$ meet) joined to the three internal vertices of each pentagon by an edge. In other words, the hexagon (six vertices and six edges) becomes a 'Y' shape on its side (four vertices and three edges). This has been highlighted in bold in Figure 2.

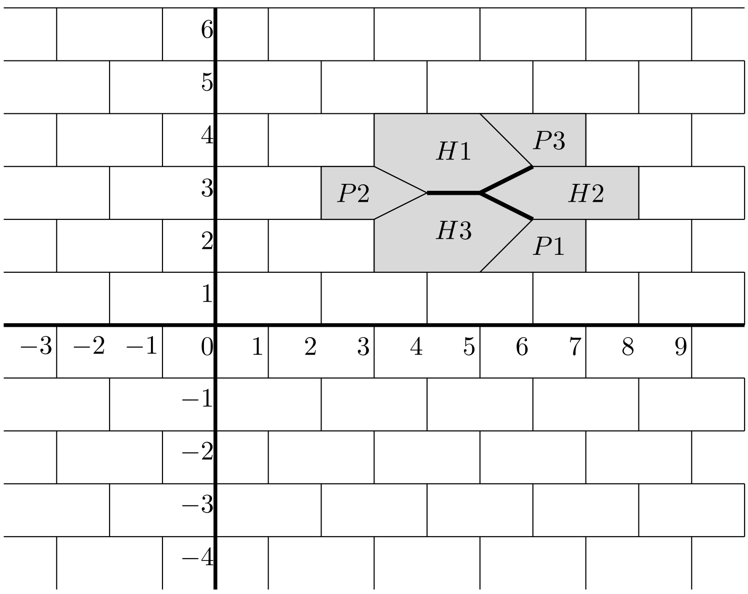

Figure 2: A wall model containing the $V_2(555-777)$ defect

Recall the following definition and theorems from [5].

Definition 2.1. Let R be a reference point on the rectangular grid. We define S to be the length of the shortest closed path with odd length starting and ending at R.

Theorem 2.2. *Let R be positioned at the top of a vertical line, then*

a) R lies in region A if and only if $S \equiv 1 \pmod 4$,

b) R lies in region B if and only if $S \equiv 3 \pmod 4$.

Theorem 2.3. *Let R be positioned at the bottom of a vertical line, then*

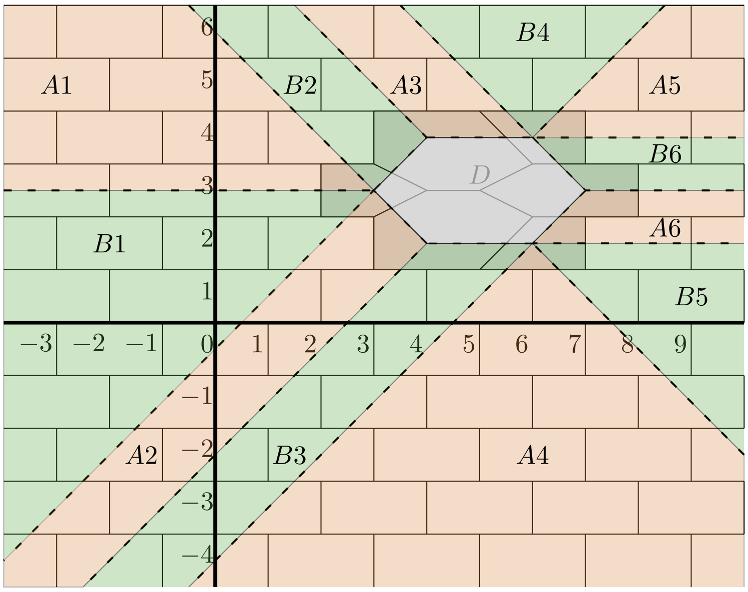

Figure 3: Regions of a wall model for a $V_2(555-777)$ defect

a) R lies in region A if and only if $S \equiv 3 \pmod 4$,

b) R lies in region B if and only if $S \equiv 1 \pmod 4$.

We will denote by Si the length of the shortest path of odd length starting and ending at the reference point Ri, $i = 1, 2, 3$.

Theorem 2.4. *Given* $S1$ *and then obtaining* $S2$ *(by moving the detector to the right by* $S1+1$ *units) and in some cases* $S3$ *(by moving the detector left by* $S1+1$ *units) it is possible to determine in which region the detector was initially placed i.e., in which region* $R1$ *lies.*

Proof. (a) Suppose that $S1$ and $S2$ are both congruent to $1 \pmod 4$. If

(i) $S2 = 2S1 + 3$, then $R1$ is in $A3$ and $R2$ in $A5$,

(ii) $S2 < 2S1 + 3$, then $R1$ is in $A1$ and $R2$ in $A5$.

(b) If $S1$ and $S2$ are both congruent to $1 \pmod 4$ and $S2 = 3S1 + 2$, then $R1$ is either in $A5$ or in $A6$ and $R2$ is getting further away from the break. Thus instead move the detector $S1 + 1$ units to the left of $R1$ to position $R3$. Then

(i) $S3 \equiv 1 \pmod 4$ implies that $R1$ is in $A5$ (and thus $R3$ is in $A1$),

(ii) $S3 \equiv 3 \pmod 4$ gives $R1$ is in $A6$ (and so $R3$ is in $B1$).

(c) When $S1 \equiv 1 \pmod 4$ and $S2 \equiv 3 \pmod 4$ and

(i) $S2 = 2S1 - 3$ then $R1$ is in $A2$ and $R2$ in $B5$,

(ii) $S2 > 2S1 - 3$ then $R1$ is in $A4$ and $R2$ in $B5$.

(d) If $S1 \equiv 1 \pmod 4$ and $S2 \equiv 3 \pmod 4$ and if $S2 = S1 + 2$ then $R1$ is in $A1$ and $R2$ is in $B6$.

(e) Suppose that $S1$ and $S2$ are both congruent to $3 \pmod 4$. Then

  (i) $S2 = 2S1 + 1$ implies that $R1$ is in $B3$ and $R2$ in $B5$,

  (ii) $S2 < 2S1 + 1$ gives that $R1$ is in $B1$ and $R2$ in $B5$.

(f) When $S1$ and $S2$ are both congruent to $3 \pmod 4$ but $S2 = 3S1 + 2$, then $R1$ is either in $B5$ or in $B6$ and $R2$ is further away from the break than $R1$. As in (b) move the detector to $R3$. If

  (i) $S3 \equiv 1 \pmod 4$ then $R1$ is in $B6$ (and thus $R3$ is in $A1$),

  (ii) $S3 \equiv 3 \pmod 4$ then $R1$ is in $B5$ (and $R3$ is in $B1$).

(g) Assume that $S1 \equiv 3 \pmod 4$ and $S2 \equiv 1 \pmod 4$. If

  (i) $S2 = 2S1 - 1$ then $R1$ is in $B2$ and $R2$ in $A5$,

  (ii) $S2 > 2S1 - 1$ then $R1$ is in $B4$ and $R2$ in $A5$.

(h) If $S1 \equiv 3 \pmod 4$ and $S2 \equiv 1 \pmod 4$ and $S2 = S1 + 2$ then $R1$ is in $B1$ and $R2$ is in $A6$.

■

3 Symmetry

In this section we introduce three groups of regions which we will prove are symmetrical about the break by a rotation of 120 degrees (with respect to the hexagonal grid). The nodes within regions $A2, B1, A1$ and $B2$ are in the base group, called Group 1. The nodes in regions $A3, B4, A5$ and $B6$ are in Group 2. The nodes in regions $A6, B5, A4$ and $B3$ are in Group 3.

We will use the variable n to aid in the navigation between the triangular regions in these three groups. The value of n indicates how far we are from the boundary with the other triangular region in the same group. More specifically, all nodes closest to the boundary between $A1$ and $B1$ will have an n value of zero. Considering nodes, with the same $S1$, further away from this boundary, n increases by 2 for every two edges traversed between nodes. Equivalently, all nodes closest to the boundary between $A5$ and $B4$, as well as the boundary between $A4$ and $B5$, will have an n value of 0. For example, in Figure 3, the point $(8, -1)$ in region $A4$ has an n value of 0 (and an $S1$ value of 13), and the corresponding points in $A5$ and $A1$ are $(9, 6)$ and $(-2, 3)$ respectively. For $S1 = 13$ and $n = 4$ in $A4$, the coordinates are $(4, -1)$ and the corresponding points in $A5$ and $A1$ are $(11, 4)$ and $(0, 5)$ respectively. The formulae to find explicit values of n are provided in Corollary 3.2.

Theorem 3.1. *The nodes within Group 1 are symmetrical about the break, by a clockwise rotation of 120 degrees (in the hexagonal grid), with the nodes in Group 2. Equivalent vertices in Group 3 are obtained by a further 120 degrees clockwise rotation. Explicit formulae for this symmetry between equivalent nodes in the rectangular grid exist in terms of $S1$ and n.*

Proof. Note that the symmetry is with respect to the shortest paths and in the rectangular grid is given in terms of movements vertically and horizontally. In the rectangular grid in Figure 3, the rotation is about the point $(5, \frac{5}{2})$, but is not generally 120 degrees.

We will show that a vertex $R1$ at the top of a vertical line in region $A3$ (respectively $B4$, $A5$, $B6$) has a unique image called $R1'$ in $A2$ (respectively $B1$, $A1$, $B2$). Similarly a vertex $R1$

in region $A6$ at the top of a vertical line (respectively $B5$, $A4$, $B3$) corresponds to a unique vertex $R1'$ in $A2$ (respectively $B1$, $A1$, $B2$). We give the formulae for moving from a node $R1$ in Group 2 or 3 to the equivalent node $R1'$ in Group 1. A detailed explanation is given for finding the corresponding nodes in regions $A6$ and $B5$ to those in regions $A2$ and $B1$ respectively, while the other transformations follow the same argument.

(a) Consider the node with $S1 = 5$ in $A6$ and the corresponding node in $A2$. To move from the former to the latter requires a shift of 4 units to the left and 0 units down.

For an arbitrary node $R1$ with coordinates (x_1, y_1) in $A6$, when $S1$ increases by 4, we move within $A6$ two units to the right, i.e., to the coordinates (x_1+2, y_1) and within $A2$ we move one unit left and one unit down, i.e., from the point (x_2, y_2) to the point (x_2-1, y_2-1). Thus the corresponding shift from $A6$ to $A2$ increases by 3 units to the left and 1 unit down (compared to the shift for the smaller/previous $S1$).

Therefore, for any node in $A6$ we go left by $\frac{3S1+1}{4}$ units and down by $\frac{S1-5}{4}$ units to reach the corresponding node in $A2$.

(b) For $n = 0$, when moving in $B5$ from some node with $S1$ to the node with $S1 + 4$ and $n = 0$ we are moving one unit down and one unit to the right, while in $B1$ the equivalent movement is given by moving two units to the left. This is because in the rectangular grid, the vertical edges (in $B5$) become horizontal edges in $B1$ (based on the original rotation in the hexagonal grid). In a similar manner, the horizontal edges in $B5$ that are immediately to the right of the top of the vertical line become vertical edges in $B1$.

First, note that the smallest $S1$ value in $B5$ is 7 and to move from that node to the corresponding node in $B1$, we move left by 7 units and up by 1 unit.

Now inductively, for any node in $B5$ where $n = 0$, denoted by (x_1, y_1), if we increase $S1$ by 4 this corresponds to moving to the node (x_1+1, y_1-1). The equivalent change in $B1$ is from the node (x_2, y_2) to the node (x_2-2, y_2). This means that the horizontal change (to the left) when moving from $B5$ to $B1$ is increased by three units. Similarly, when moving from $B5$ to $B1$ there is a vertical increase by one (up). So the linear relation between $S1$ and the number of steps to the left is given by $\frac{3S1+7}{4}$ and the number of steps up is $\frac{S1-3}{4}$.

In $B5$ the nodes on the border with $A4$ correspond to $n = 0$. Then n increases by 2 each time we move one unit right and one unit up to the next vertex with the same $S1$ value in $B5$.

For a fixed $S1$ if the node in $B5$ with $n = 0$ is (x_1, y_1) then the coordinates of the other nodes with the same $S1$ are given by $(x_1+\frac{n}{2}, y_1+\frac{n}{2})$ and recall that we increment n by 2. The corresponding nodes in $B1$ have coordinates (x_2, y_2) and $(x_2+\frac{n}{2}, y_2-\frac{n}{2})$. Thus the horizontal change is the same as for $n = 0$, i.e. $\frac{3S1+7}{4}$. Now, the difference in the second coordinate for nodes in $B5$ is $\frac{n}{2}$ while for the nodes in $B1$ this difference is $-\frac{n}{2}$, this leads to a change of $-n$ in the vertical shift. Hence the total vertical shift is $\frac{S1-3}{4} - n$. Note that for large values of n this may be negative, in which case the movement is downwards.

Hence, for any node in $B5$, we move left by $\frac{3S1+7}{4}$ and up by $\frac{S1-3}{4} - n$ to reach the equivalent node in $B1$.

(c) Consider the nodes in $A4$ on the border of $B5$ (right-most nodes in $A4$). For these nodes let $n = 0$ and let n increase by 2 for each movement along two edges to the left. Note that this node is also at the top of a vertical line. To get to the corresponding node in $A1$, we shift $\frac{3S1+1}{4} - \frac{3}{2}n$ units to the left and $\frac{S1+3}{4} + \frac{n}{2}$ units up.

(d) For any node in $B3$, the corresponding node in $B2$ is given by going 1 unit to the left and $\frac{S1-1}{2}$ units up.

(e) To get from a node in $A3$ to the equivalent node in $A2$ we shift 2 steps to the left and $\frac{S1-1}{2}$ steps down.

(f) In $B4$, $n = 0$ for the nodes closest to the boundary with $A5$. To get from a node in $B4$ to the corresponding node in $B1$ we go $\frac{3S1-1}{4} - \frac{3}{2}n$ units to the left and $\frac{S1+5}{4} + \frac{n}{2}$ units down.

(g) To translate nodes from $A5$ to $A1$, recall that $n = 0$ for the nodes closest to the border with $B4$, we shift $\frac{3S1+5}{4}$ steps to the left and $\frac{S1-1}{4} - n$ steps down (for negative values this would mean going up).

(h) Finally, when moving from vertices in $B6$ to equivalent vertices in $B2$ we go left by $\frac{3S1-1}{4}$ units and up by $\frac{S1-3}{4}$ units.

■

The following result can be obtained using the same technique as in the proofs of (a) and (b) in the above theorem, since the pairings of $S1$ and $S2$ (respectively $S1$ and $S3$) are unique. Note that the n values defined prior to Theorem 3.1 are only required in regions $A4$, $B4$, $A5$ and $B5$ since the other regions are either strips with no repeated $S1$ values or are in Group 1.

Corollary 3.2. *The n values in terms of $S1$ and $S2$ (or $S3$) are given by the following expressions. For region*

- *$B5$, $n = \frac{2S1-S3-3}{2}$,*
- *$A4$, $n = \frac{3S1-S2}{2}$,*
- *$B4$, $n = \frac{3S1-S2}{2}$ and*
- *$A5$, $n = \frac{2S1-S3-1}{2}$.*

Thus, if we are in any of the regions of Group 2 or Group 3 and we have $S1$ and $S2$ (or $S3$) then we know n. Consequently, we can give what the value of $S2$ would be if we moved from the equivalent node in Group 1 by $S1 + 1$ units to the right. We denote this by $S2'$ and then we can apply the algorithm below with $S2$ replaced by $S2'$. For vertices in

- *$A3$ or $A6$, $S2' = 2S1 - 3$ if $S1 > 5$ otherwise $S2' = 9$,*
- *$B3$ or $B6$, $S2' = 2S1 - 1$ and*
- *$A4$, $A5$, $B4$ or $B5$, $S2' = S1 + 2n$ when $n \neq 0$ and $S2' = S1 + 2$ when $n = 0$.*

4 Algorithm to locate the break

Consider a reference point positioned at the top of a vertical line in Group 1 ($A2, B1, A1$ or $B2$). The following algorithm locates the break uniquely by determining the point labelled D in Figure 3. Note that if the reference point is in Group 2 or 3, then we use $S2'$ (see Corollary 3.2) instead of $S2$ in this algorithm.

Algorithm 4.1. Determining uniquely the coordinates of D for a $V_2(555 - 777)$ defect.

1) Label point $R1$ (which is at the top of a vertical line) as the origin, i.e., $R1(0,0)$. Note that this $R1$ is not the same origin (used to illustrate the rectangular grid) in Figure 2 and Figure 3.

2) Select a second reference point $R2$ by moving $S1+1$ units horizontally to the right of $R1$, i.e., the coordinates of $R2$ are $(S1+1,0)$. Now $S2$, which is either 1 (mod 4) or 3 (mod 4), can be obtained experimentally from the detector.

3a) If $S1 = 5$ and $S2 = 9$ then $R1$ is in $A2$ (it is on the break) and $R2$ is in $A6$. The coordinates of D are $(2, \frac{1}{2})$.

3b) If $S1 \equiv 1 \pmod 4$, $S2 \equiv 1 \pmod 4$ and $S1 > 5$, then $R1$ is in $A1$ and $R2$ is in $A5$. The coordinates of D are $(\frac{3S1-S2+2}{4}, -\frac{S2-S1+2}{4})$.

4) If $S1 \equiv 3 \pmod 4$, $S2 \equiv 3 \pmod 4$ and $S1 > 5$, then $R1$ is in $B1$ and $R2$ is in $B5$. The coordinates of D are $(\frac{3S1-S2+2}{4}, \frac{S2-S1+2}{4})$.

5a) If $S1 \equiv 1 \pmod 4$, $S2 \equiv 3 \pmod 4$ and $S2 = S1+2$, then $R1$ is in $A1$ and $R2$ is in $B6$. The coordinates of D are $(\frac{S1+1}{2}, -\frac{1}{2})$.

5b) If $S1 \equiv 1 \pmod 4$, $S2 \equiv 3 \pmod 4$ and $S2 > S1+2$, then $R1$ is in $A2$ and $R2$ is in $B5$. The coordinates of D are $(\frac{S1+3}{4}, \frac{S1-3}{4})$.

6a) If $S1 \equiv 3 \pmod 4$, $S2 \equiv 1 \pmod 4$ and $S2 > S1+2$, then $R1$ is in $B2$ and $R2$ is in $A5$. The coordinates of D are $(\frac{S1+1}{4}, -\frac{S1-1}{4})$.

6b) If $S1 \equiv 3 \pmod 4$, $S2 \equiv 1 \pmod 4$ and $S2 = S1+2$, then $R1$ is in $B1$ and $R2$ is in $A6$. The coordinates of D are $(\frac{S1+1}{2}, \frac{1}{2})$.

Note. The algorithm gives the coordinates of D from Group 1. If $R1$ was not in Group 1 then we need to change/compensate to get D relative to the original reference point in Group 2 or Group 3 using Theorem 3.1.

5 Example

Assume we are given $S1 = 15$ and $S2 = 47$ from detectors placed at $R1$ and $R2$ respectively. Both are 3 (mod 4) so part (f) of Theorem 2.4 applies. Thus, moving to the left and placing the detector at $R3$ we get $S3 = 23$ which is also 3 (mod 4). Hence $R1$ is in $B5$. The equivalent point to $R1$ in $B1$ is denoted by $R1'$ and has coordinates $(-13, 1)$ and this consequently gives an $R2'$ by moving 16 units to the right, see Figure 4. From Corollary 3.2 we find $n = 2$ and thus $S2' = 19$. Using part 4) of Algorithm 4.1 with $S2$ replaced by $S2'$ gives the coordinates of D as $(7, \frac{3}{2})$ relative to $R1'$. Lastly, we need to shift accordingly to find D from the initial origin at $R1$ in $B5$ which is done using part (b) of Theorem 3.1. Thus we shift $\frac{3S1+7}{4} = 13$ units to the left and $\frac{S1-3}{4} - n = 1$ unit up. Thus $D = (-6, \frac{5}{2})$. This example is demonstrated in Figure 4, where the solid blue closed path has length $S1$ and the solid red closed path has length $S3$. The dotted blue and red closed paths indicate $S1'$ and $S2'$ respectively.

In summary, given a graphene nano-ribbon containing at least one $V_2(555-777)$ defect, the algorithm uses only the electrical properties of graphene to determine the exact position of the $V_2(555-777)$ defect closest to the initial position of the detector. These defects affect the properties of the pristine system, which can be beneficial or detrimental from the application point of view. The above could be utilised in patching (i.e., mending) such defects where it would be necessary first to know the position of the defect.

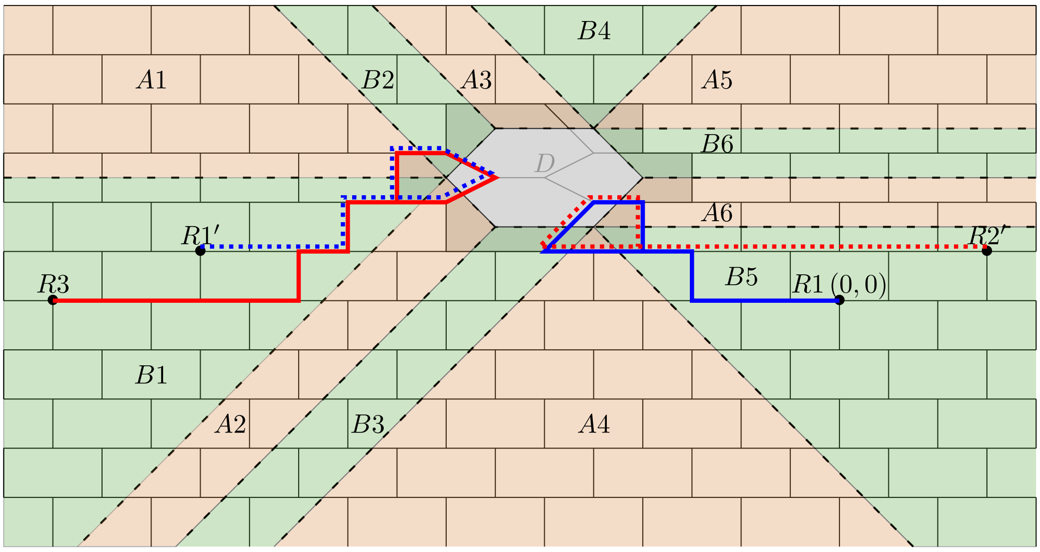

Figure 4: Example of locating a $V_2(555-777)$ defect

Conflicts of Interest. The authors declare that they have no conflicts of interest regarding the publication of this article.

References

[1] B. Zheng and G. X. Gu, Machine learning-based detection of graphene defects with atomic precision, *Nano-Micro Lett.* 12 (181) (2020) 1–13, https://doi.org/10.1007/s40820-020-00519-w.

[2] N. Jing, Q. Xue, C. Ling, M. Shan, T. Zhang, X. Zhoub and Z. Jiao, Effect of defects on Young's modulus of graphene sheets: a molecular dynamics simulation, *Rsc Advances* 2 (2012) 9124–9129, https://doi.org/10.1039/C2RA21228E.

[3] W. Tian, W. Li, W. Yu and X. Liu, A review on lattice defects in graphene: types, generation, effects and regulation, *Micromachines* (Basel) 8 (5) (2017) p. 163, https://doi.org/10.3390/mi8050163.

[4] L. Vicarelli, S. J. Heerema, C. Dekker and H. W. Zandbergen, Controlling defects in graphene for optimizing the electrical properties of graphene nanodevices, *ACS Nano* 9 (4) (2015) 3428–3435, https://doi.org/10.1021/acsnano.5b01762.

[5] M. Archibald, S. Currie and M. Nowaczyk, Finding the hole in a wall, *J. Math. Chem.* 58 (2020) 2313–2323, https://doi.org/10.1007/s10910-020-01178-3.

[6] M. Archibald, S. Currie and M. Nowaczyk, Locating a double vacancy or Stone-Wales point defect on a hexagonal quantum grid, *J. Math. Chem.* 60 (2022) 862–873, https://doi.org/10.1007/s10910-022-01337-8.

[7] B. Gutkin and U. Smilansky, Can one hear the shape of a graph?, *J. Phys. A: Math. Gen.* 34 (2001) 6061–6068, https://doi.org/10.1088/0305-4470/34/31/301.

[8] P. Kurasov and M. Nowaczyk, Inverse spectral problem for quantum graphs, *J. Phys. A: Math. Gen.* 38 (2005) 4901–4915, https://doi.org/10.1088/0305-4470/38/22/014.